Coral Reefs (2001) 20: 387–398
DOI 10.1007/s00338-001-0188-3

REPORT

Kazuo Nadaoka · Yasuo Nihei · Ryoko Kumano
Tatsuya Yokobori · Tatsuo Omija · Kensui Wakaki

A field observation on hydrodynamic and thermal environments of a fringing reef at Ishigaki Island under typhoon and normal atmospheric conditions

Received: 20 March 2001 / Accepted: 12 July 2001 / Published online: 7 November 2001

Abstract To investigate the hydrodynamic and thermal environments of a fringing coral reef under possible influences from both inland and offshore, we have conducted a field survey at Shiraho reef on Ishigaki Island, Okinawa, Japan, by deploying 16 moored buoys inside and outside the reef, on which various sensors for continuous measurements of water temperature, salinity, and turbidity concentration were installed. Several bottom-mounted current meters and wave gauges were also deployed. The results show the abrupt decrease and increase of the water temperature during a typhoon, with the resultant temperature being about 1 degree lower than before. The main cause of this abrupt change and the difference between inside and outside the reef in the thermal response to the atmospheric agitation are investigated. For normal atmospheric conditions, the overall characteristics of currents in the coral reef are found to be governed by the dynamic balance among tide, waves, and wind effects. The salinity and turbidity variations near the river mouth and their cause are also investigated. Thermal environment in the reef is examined by a heat-budget analysis, indicating that it is influenced by both the atmospheric conditions and the temperature difference between inside and outside the reef.

Keywords Fringing reef · Hydrodynamic and thermal environments · Water temperature fluctuation · Heat-budget analysis · Influences from land and offshore · Typhoon

K. Nadaoka (✉) · K. Wakaki
Department of Mechanical and Environmental Informatics,
Tokyo Institute of Technology, 2-12-1, Ookayama,
Meguro-ku, Tokyo 152-8552, Japan
E-mail: nadaoka@mei.titech.ac.jp

Y. Nihei
Department of Civil Engineering,
Science University of Tokyo, 2641 Yamazaki,
Noda-shi, Chiba 278-8510, Japan

R. Kumano
Fukui Prefectural Government, 42-2-1 Kamiohta-cho,
Takefu-shi, Fukui 915-0882, Japan

T. Yokobori
Tokyo Metropolitan Government, 5-1-1 Nakagawa,
Adachi-ku, Tokyo 120-0002, Japan

T. Omija
Okinawa Prefectural Institute of Health and Environment,
2085 Aza-ozato, Ozato-mura,
Okinawa 901-1202, Japan

Introduction

The Ryukyu Islands, which are located at the southwestern part of Japan and mostly encompassed by well-developed fringing reefs, have been subjected to various land-based environmental impacts such as sediment pollution. Mass coral bleaching, which occurred globally in 1998, also was observed in the Ryukyu Islands (e.g., Research Institute for Subtropics 1999; Yamazato 1999). The occurrence of bleaching and resultant mortality of corals exhibited appreciable variability on various scales, on the global, regional, reef, and community scale. One of the possible causes of the spatial non-uniformity of the coral bleaching and mortality is the variability of the water temperature in the ocean in various scales. However, even in the case of uniform condition of the offshore water temperature, a variability may still arise in coral bleaching and mortality on the regional scale or smaller. This may be caused by, e.g., local topographic effects on the reef scale, which may influence the connection of the thermal environments in the reef with those outside the reef. Sedimentation may provide an additional cause of the spatial non-uniformity of coral bleaching and mortality on the regional scale or smaller (e.g., Hasegawa et al. 1999).

For detailed and quantitative understanding of actual physical processes governing these phenomena, we need to know the hydrodynamic and thermal environments in reefs, with special emphasis on the connections

with offshore and terrestrial waters in various conditions. However, these have not been well understood, although various knowledge on the current and sedimentary process in reefs has been compiled in previous studies (e.g., Andrews and Pickard 1990; Wolanski 1994).

For the Ryukyu Islands, Tanimoto et al. (1988) and Nakaza et al. (1992a, 1992b, 1994a) made field observations on wave and current fields in the Okinawa reefs. Nakamori et al. (1992), Okinawa Environmental Technology Association (1996), and Yamano et al. (1998) performed field measurements on circulation in the coral reefs at Ishigaki Island. Further, the advective diffusion and deposition of fine sediments in the reefs have been studied by Tsukayama et al. (1992), Nakaza et al. (1994b), and Omija (1996). However, little has been known on the hydrodynamic and thermal process in the reef in the context of their connections with offshore and terrestrial waters. Especially, in the conditions of episodic atmospheric agitation like typhoons, the hydrodynamic and thermal influences from offshore and rivers remain unknown.

Therefore, in this study, we have attempted to clarify the hydrodynamic and thermal environments of coral reefs and their relationships with the water environments outside the reef and of river plume. For this purpose, we conducted a field study at Shiraho reef at the Ishigaki Island, Okinawa, by deploying various sensors inside and outside the reef for continuous measurements of water temperature, salinity, turbidity, and chlorophyll *a* concentration as well as current and waves.

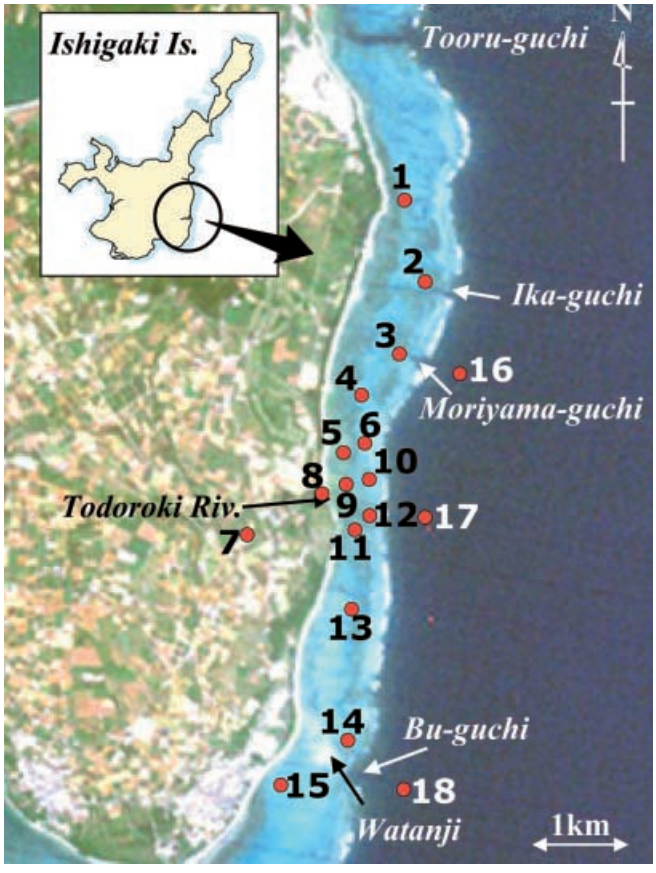

Fig. 1 LANDSAT/TM image of Shiraho coral reef, Ishigaki Island, Japan, and measuring stations where sensors were deployed with a moored buoy system or others

Methods

Field observation

Study site

The field observation was performed at Shiraho Reef located on the east coast of Ishigaki Island in the Ryukyu Islands, Japan (Fig. 1), from 7 October to 8 November in 1998. Shiraho Reef is a well-developed fringing reef of about 800 m in width, having a typical topographic feature with moat, reef pavement, reef crest, and reef edge (Nakamori et al. 1992 ; Kayanne et al. 1995). At low tide the water depth in the moat is around 1.5 m and the reef crest is exposed. The coastal line is oriented approximately to the north and south. The observation was made on the stretch of about 8 km along the shore, in the middle of which the Todoroki river mouth is located. In the observation area, three channels called "Ika-guchi," "Moriyama-guchi," and "Bu-guchi" hydraulically connect with the outer sea. At the southern end of the observation area, there exists a shoal, "Watanji," which stretches across the reef and is exposed during low tide.

Sensor deployment

We set 18 measuring stations at the locations indicated in Fig. 1; among them, Stns. 8 and 7 were at the Todoroki River mouth and about 1 km upstream, respectively, and Stns. 16, 17, and 18 were located in the outer sea area with water depths of about 25 m. At these measuring stations, except for Stns. 7 and 8, we deployed moored buoys for installing various memory-type sensors, as illustrated in Fig. 2. Table 1 summarizes the sensor types, names, numbers, and locations; thermometers and salinometers were located at all the measuring stations; turbidity and chlorophyll *a* meters at Stns. 5, 7, 8, and 11; electronic current meters and pressure gauges for the measurements of velocity at 60 cm above the bottom, wave height, and water level at Stns. 1, 9, 10, 15, and 17; and acoustic Doppler current profiler (ADCP) at Stns. 16 and

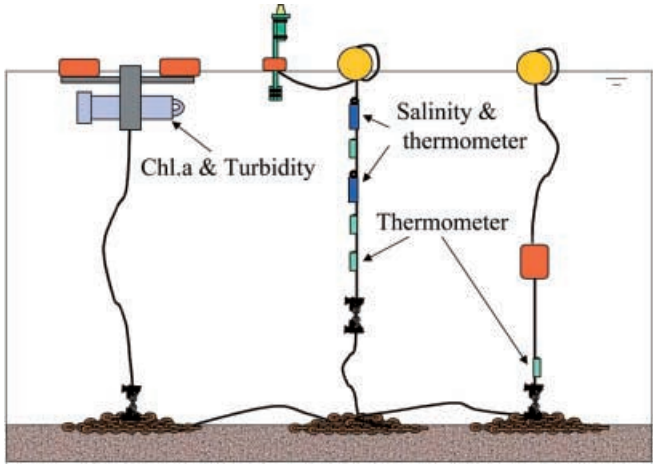

Fig. 2 Example illustration of a moored buoy system (Stn. 5)

Table 1 Sensors and their locations. *ADCP* Acoustic doppler current profiler. Manufacturers: *A* ALEC Electronics Co., Ltd.; *R* RD Instruments; *I* I-O Technique Co., Ltd.; *K* Kyowa-Shoko; *E* Eijkelkamp

Instrument	Product name (manufacturer)	Number	Locations
Thermometers	MIDS-T, MIDS-CT (*A*)	97	All
Salinometers	MIDS-CT (*A*)	31	All
Turbidity and chlorophyll *a*	ACL104–8M, ACL11–8M, ACL3–8M (*A*)	4	River and river mouth
Velocimeters	ACM–8M, ACM–8M (*A*)	3	Channel
ADCPs	Broad Band ADCP: 1,200 kHz, Work Horse ADCP: 600 kHz (*R*)	2	Outer sea
Wave gauges	Wave Hunter (*I*), DL–2, DLEP1 (*K*)	5	Reef and outer sea
Tide gauges	Diver (*E*)	4	Reef

17. (At Stns. 16, 17, and 18, the measurements were made until 31 October.) In a preliminary observation, it was found that a river plume from the Todoroki River was only several tens of centimeters thick. Therefore, for measuring the river plume, we installed vertical arrays of the thermometers and salinometers every 20 cm near the water surface, and the turbidity and chlorophyll *a* meter at about 20 cm below the water surface (Fig. 2).

Results and discussion

Meteorological and oceanographic states during the observation

Meteorological state

Figure 3 shows the time variations of the wind vector, air temperature, solar radiation, precipitation, atmospheric pressure corrected as the value at the mean sea level, and vapor pressure during the observation period from 7 October to 8 November 1998. The wind field was dominated by northeast wind of about 5 m/s except for the period from 15 to 17 October, during which typhoon no. 9810 passed by the west of Ishigaki Island, resulting in the strong wind of more than 20 m/s with the clockwise rotation as indicated in the hatched area in Fig. 3. The air temperature and the vapor pressure decreased from 16 October and remained lower by average subsequently for several days. Although the solar radiation decreased with the atmospheric pressure in the period of this typhoon passage, the precipitation was not so appreciable, and therefore the river discharge at the Todoroki River was only two or three times larger than usual. On the other hand, on 31 October, a large flood was observed with precipitation of more than 30 mm/h (Fig. 4).

Sea state

Figure 5 shows the time variation of the mean water level at Stn. 1 as a typical example of the mean water level fluctuation in the reef, which indicates that the tidal range is about 1.5 m at the spring tide and about 0.8 m at the neap tide, and that during the typhoon passage an abrupt increase in water level appeared in correspondence with the decrease in the atmospheric pressure.

Figure 6 shows the time history of the near-bottom velocities at Stns. 9 and 10 in the reef and of the vertically averaged horizontal velocity at Stn. 17 in the outer sea, which are indicated every 1 h. The near-bottom velocity at Stn. 9 shows large values of more than 40 cm/s in the typhoon passage, but in the other ordinary period it has no close correlation with the wind. At Stn. 10, which is only about 200 m apart from Stn. 9, the near-bottom velocity is very small even in the typhoon passage and the principal direction of the flow fluctuation is different from that at Stn. 9. This is due to the fact that Stn. 9 is located in the moat, while Stn. 10 is on a narrow sandy bottom area surrounded by the coral communities in the reef pavement. At Stn. 17 in the outer sea, on the other hand, the depth-averaged velocity shows a semi-diurnal fluctuation with an amplitude of about 20 cm/s and the shore-parallel principal axis.

Figure 7a shows the time variation of the vertically averaged water temperature at Stn. 8 at the river mouth, Stn. 9 in the moat, and Stn. 17 in the outer sea. Among these, the water temperature at Stn. 8 under the direct influence of the river water remains the lowest over the entire period of the observation. On the other hand, the water temperature at Stn. 17 has no appreciable diurnal fluctuation and shows abrupt change during only one day at the typhoon passage; i.e., it decreases about 3 °C and then increases about 2 °C, resulting in about 1 °C lower temperature after the passage of the typhoon. At Stn. 9 in the moat, the water temperature shows an abrupt change during the typhoon passage like that at Stn. 17 but with larger fluctuation, and after the typhoon passage it keeps lower values for several days with diurnal fluctuation. Similar features in the water temperature fluctuation were observed at other measuring stations in the reef. This is attributable to the shallowness of the water depth in the reef, in which the effect of the thermal transport through the water surface may appear more prominent compared with the outer sea.

Figure 7b shows the time variation of the water temperature at three different depths – near-surface, middle, and near-bottom – at Stn. 17, showing the presence of the slight temperature stratification during the period, except for the typhoon passage, in which the strong vertical mixing may destroy the stratification. In

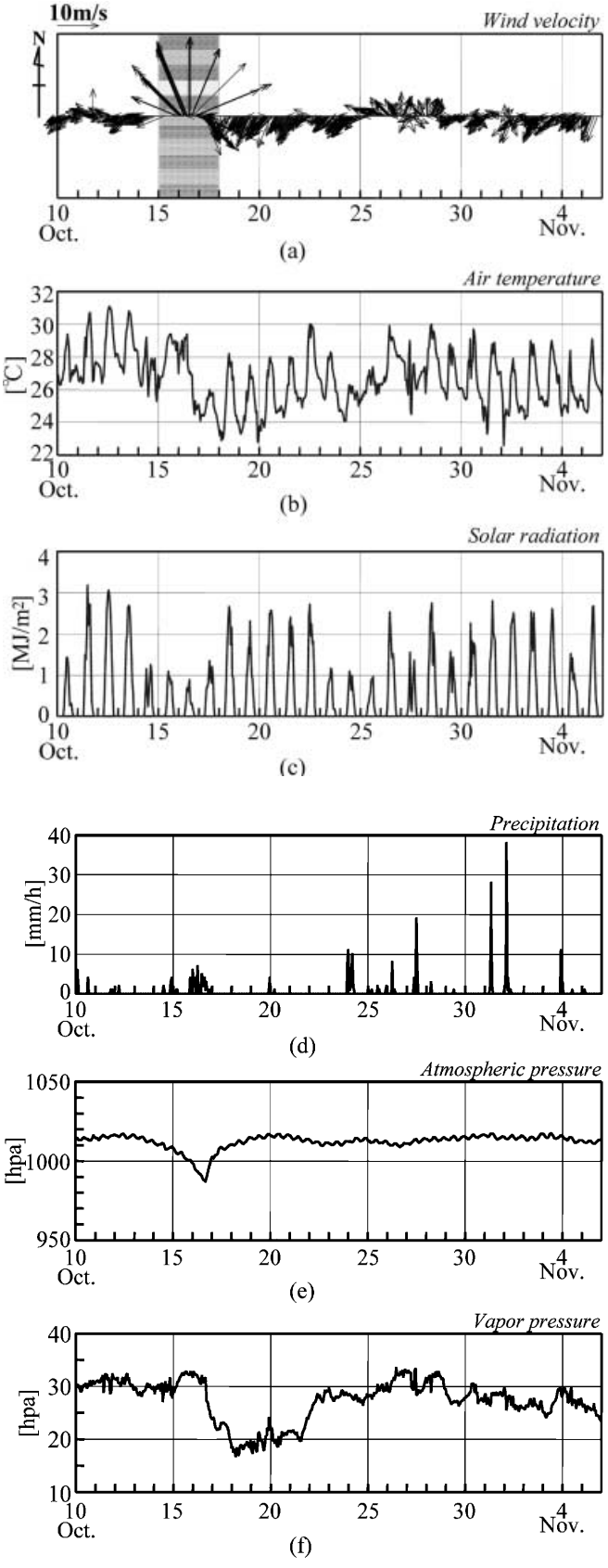

Fig. 3 Time variations of meteorological data: **a** wind velocity; **b** air temperature; **c** solar radiation; **d** precipitation; **e** atmospheric pressure; **f** vapor pressure

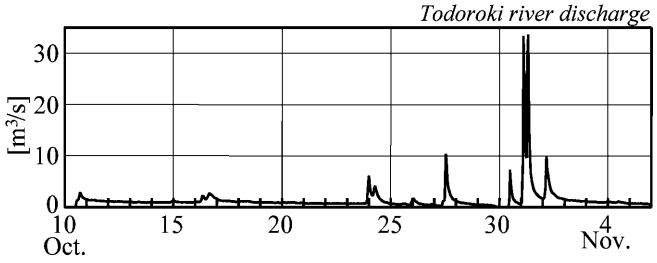

Fig. 4 Discharge at Todoroki River

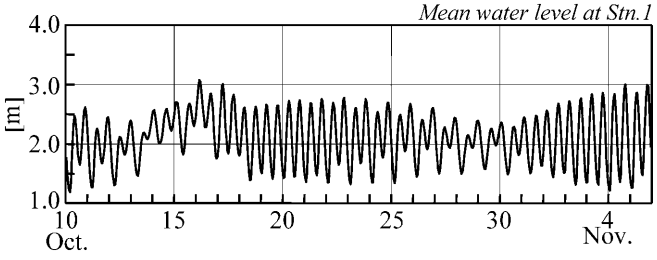

Fig. 5 Time series of mean water elevation at Stn. 1

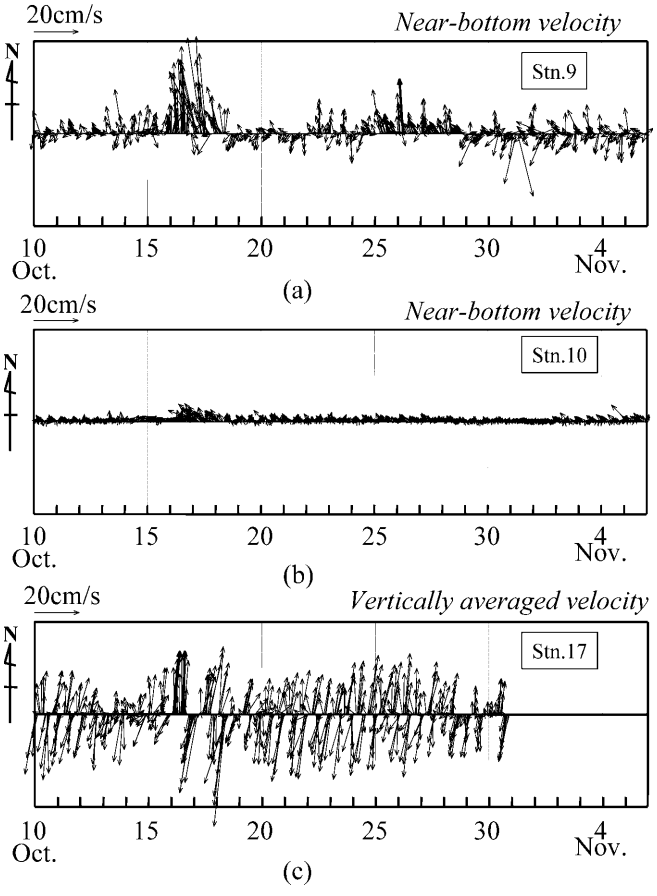

Fig. 6 Current velocity vectors inside and outside the reef. Near-bottom current velocity at **a** Stn. 9 and **b** Stn. 10, and **c** vertically-averaged velocity at Stn. 17

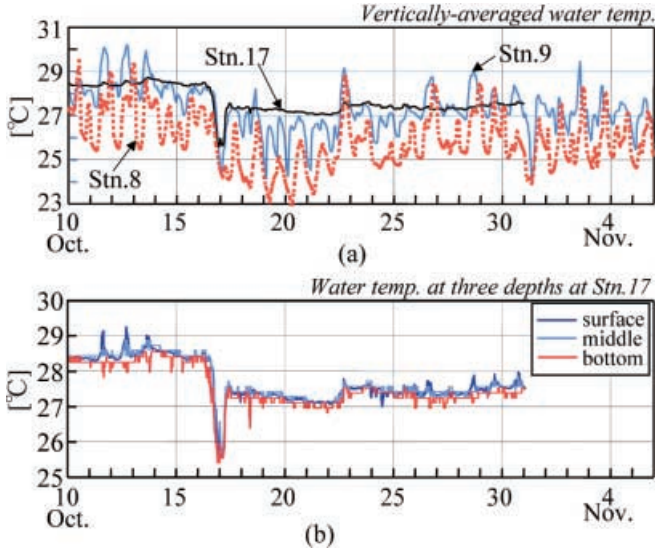

Fig. 7 Time sequences of water temperature. **a** Fluctuations of vertically averaged water temperature inside and outside the reef; **b** water temperature at three different depths at Stn. 17

the reef, appreciable temperature stratification was not observed except for the period of the big flood on 31 October.

Hydraulic and thermal environments during typhoon

Abrupt change in water temperature during typhoon

Figure 8 gives more detailed presentation of the vertically averaged temperature variation during the typhoon passage at Stn. 17 in the outer sea, Stn. 9 in the moat in front of the river mouth, and Stn. 15 located at the southernmost part of the observation area. Although the temperatures at Stns. 9 and 15 in the reef exhibit a similar abrupt decrease and subsequent increase pattern, appreciable differences may also be found in the lowest temperature and the times from which the subsequent temperature rise appears. This is a good example that shows that the dynamic response of the water temperature change in the reef against an episodic atmospheric agitation like typhoon may vary with the location in the reef.

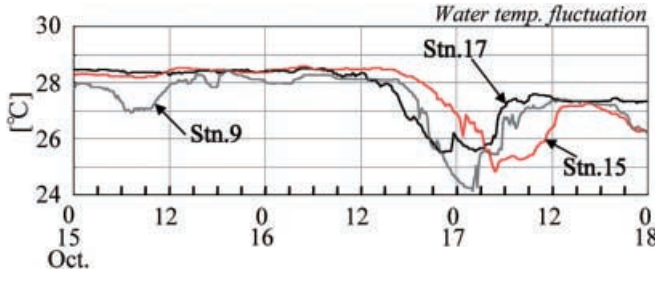

Fig. 8 Water temperature fluctuations during passage of the typhoon

For more detailed investigation of these abrupt changes in the water temperature both inside and outside the reef, we have attempted a heat-budget analysis for these three locations. The equation representing the heat balance for a water column with a unit horizontal area is:

$$\dot{Q} = G + \Delta F + G_{soil} \tag{1}$$

in which $\dot{Q}$ represents the temporal change rate of the heat storage in the water column, G denotes the heat flux through the water surface, ΔF is the contribution of the horizontal flux due to horizontal advection and diffusion, and G_{soil} indicates the heat flux through the sea bottom. In the following discussions, each flux in Eq. (1) is represented as the value divided by the water depth for removing their dependence on the water depth, and ΔF is simply referred to as "horizontal advective flux."

Among these fluxes, $\dot{Q}$ was calculated with the measured water temperature data, and the heat flux G was estimated with the observed atmospheric data. Supposing that the vertical advective heat transfer due to the groundwater movement is negligible, G_{soil} may be evaluated as:

$$G_{soil} = \lambda \left.\frac{\partial T}{\partial z}\right|_{z=0} \tag{2}$$

where λ is the heat conduction coefficient, T is the water temperature, and z is the vertical coordinate with the origin at the sea bottom being positive downward. Since we made no measurement of T in the sea bottom, we have evaluated G_{soil} with the analytical solution of the one-dimensional thermal conduction equation for a uniform media with the time-varying temperature $T_0(t)$ at $z = 0$:

$$T(z,t) = \int_0^t \frac{z}{2\sqrt{\pi\lambda(t-\xi)^3}} \exp\left(-\frac{z^2}{4\lambda(t-\xi)}\right) T_0(\xi)\, d\xi \tag{3}$$

In the derivation of this solution, the initial temperature was assumed to be vertically uniform with the value equal to the initial sea-bottom temperature. Since a preliminary observation showed that the temperature value obtained at 20 cm above the sea bottom was found nearly the same as that at the sea bottom, the former value was given for $T_0(t)$. As the heat conduction coefficient λ, 1.071 W m^{-1} K^{-1} was given by a laboratory measurement for the coral sands as one of the typical bottom materials in the observation site.

Figure 9 shows the heat fluxes G and ΔF so obtained, which were found to dominate $\dot{Q}$. In the outer sea, the atmospheric effect G is negligibly small, while in the reef, G is comparable to the horizontal advective flux ΔF and acts to cool the water body during this period. The appearance of the positive and negative peaks of ΔF for Stns. 9 and 15 at different times suggests the presence of appreciable local topographic effects on the advective

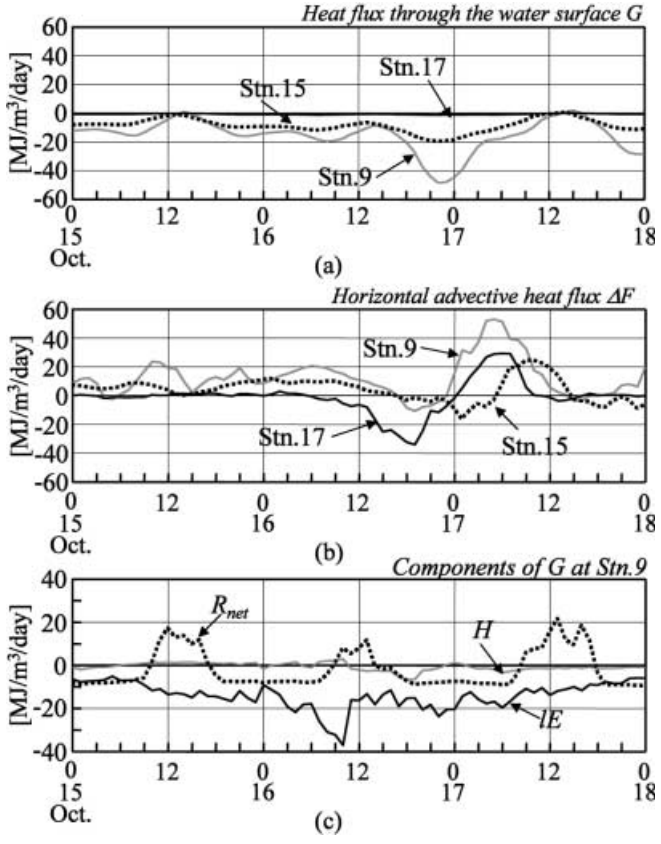

Fig. 9 Results of heat-budget analysis. **a** Heat flux through the water surface G; **b** horizontal advective heat flux ΔF; **c** components of G at Stn. 9

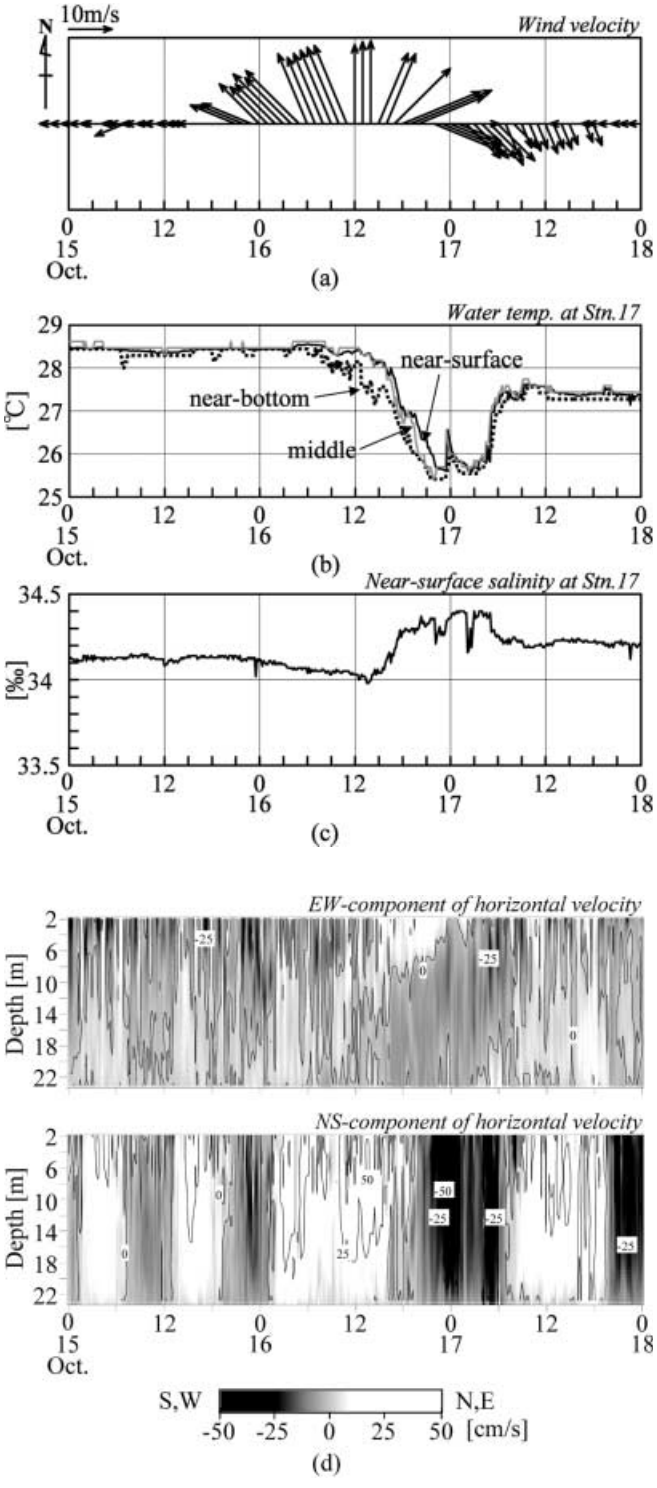

Fig. 10 Dynamic features of water temperature, near-surface salinity, and current variations outside the reef (Stn. 17) with wind vectors in the typhoon. **a** Wind velocity vector; **b** water temperature (Stn. 17); **c** near-surface salinity (Stn. 17); **d** vertical profiles of horizontal velocity (Stn. 17)

thermal transport in the reef, which may be governed by the hydrodynamics in the reef during the typhoon. The detailed analysis on this is presented in the subsequent section.

To examine the atmospheric cooling effect during the typhoon, Fig. 9c indicates three components comprising G, i.e., the net radiation R_{net}, the sensible heat flux H, and latent heat flux lE, at Stn. 9. Among these, the latent heat flux lE shows large negative values during this period, indicating that the atmospheric cooling of the reef water during typhoon was mainly due to the evaporation at the sea surface associated with the strong wind of the typhoon.

Relationship between water temperature variation and hydrodynamic processes around the reef

In the outer sea. We first examine the horizontal advective heat transport, which caused the abrupt decrease and subsequent increase in the water temperature at Stn. 17 in the outer sea during the typhoon. Figure 10a–d shows the time histories of the wind vectors, the water temperatures at three different depths, the near-surface salinity, and the vertical distributions of the EW and NS components of the horizontal velocity, respectively. The overall pattern of the salinity variation demonstrates the close relationship with that of the water temperature; i.e., the salinity increased with the decrease in the water

temperature and then abruptly decreased when the water temperature suddenly increased. The current velocity also shows close relation to these variation patterns; i.e., in the period of the temperature decrease and salinity increase, the northward current was prevailing, while in the subsequent period with the temperature increase and salinity decrease, the southward current was dominant. As illustrated in Fig. 11, the former corresponds to the coastal upwelling mode, in which the upwelling motion of the water mass with relatively low temperature and high salinity toward the reef may develop as the compensation for the Ekman transport of the surface water toward offshore, and the latter corresponds to the downwelling mode, where as the process opposite to the upwelling the surface water with relatively high temperature and low salinity may be transported toward the reef.

It is noteworthy that after the typhoon passage, water temperature and salinity attained stable levels, which were about 1 °C lower and 0.1 to 0.2‰ higher than those before the typhoon passage. To find the spatial extent of the temperature decrease in the water temperature, we examined sea surface temperature (SST) obtained by National Oceanic and Atmospheric Administration–advanced very high resolution radiometer (NOAA-AVHRR) image. Figure 12a, b indicates SST distributions before and after the typhoon passage, respectively, in the area including the East China Sea, Taiwan, and Ishigaki Island. Comparing these two figures, we can find that the typhoon caused the decrease in SST of 1 to 2 °C in wide area and about 1 °C near Ishigaki Island, which is almost identical to the value observed at Stn. 17 in the outer sea as described above. From the vertical profiles

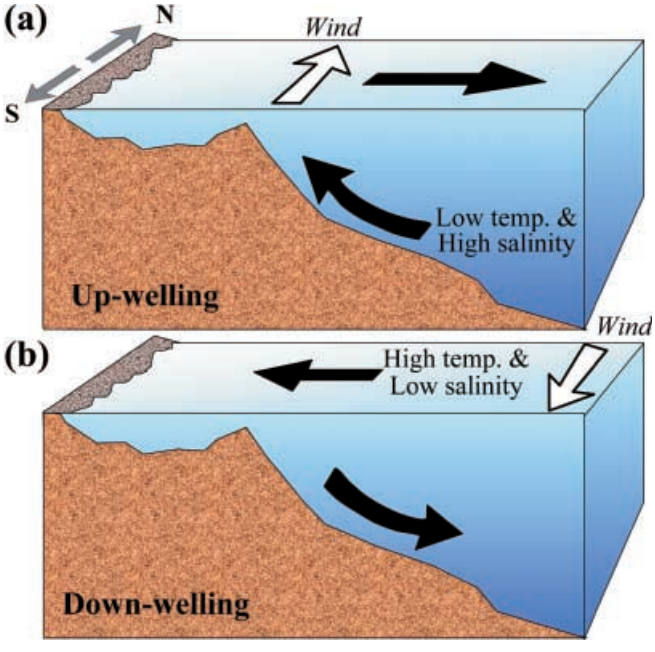

Fig. 11 Schematic illustration of **a** coastal upwelling and **b** coastal downwelling

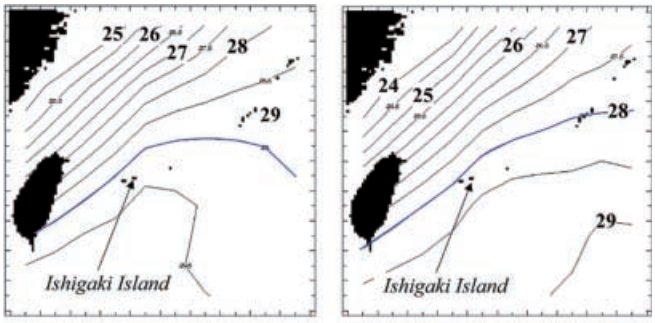

Fig. 12 Sea-surface temperature detected by NOAA-AVHRR data: **a** 14 October (before typhoon); **b** 21 October (after typhoon)

of the water temperature observed just before and after the passage of typhoon no. 9810 at Sekisei-shoko between Ishigaki and Iriomote Islands, Kuroyama et al. (1999) indicated that the surface mixing layer thickness changed from about 70 m on 12 October to about 120 m on 18 October with about 1 °C decrease in the water temperature in the surface layer. This is again consistent with our observation, and suggests that the temperature decrease by the typhoon was mainly due to the vertical mixing in the surface layer.

In the reef. Figure 13 shows the horizontal distributions of the depth-averaged temperature and near-surface salinity at 0:00 A.M. (low tide) and 6:00 A.M. (high tide) on 17 October. At low tide, the low-temperature and low-salinity water appeared near the river mouth and moved mostly toward north, indicating the effect of a river plume deflecting north. At high tide, on the other hand, the entire region of the reef was covered with the outer sea water with high salinity, but still appreciable non-uniformity can be observed especially in the water temperature distribution. This demonstrates that the effects of the river and outer sea water may appear non-uniformly in the reef.

Turbidity variations

Figure 14a,c shows the time variation of the near-surface turbidity and salinity during the typhoon at Stns. 5 and 11, which are in the moat and located in the north and south of the river mouth, respectively; and Fig. 14b indicates the near-bottom current velocity at Stn. 9 situated in between Stns. 5 and 11. At Stn. 5, the events of the salinity decrease are associated with the increase in the turbidity, indicating the effects of the turbid river plume flowing north in the reef. This is consistent with the characteristics of the water temperature and salinity distributions described in the previous section.

It should be noted, however, that at both Stns. 5 and 11 the turbidity increased also in the periods when the salinity did not show any appreciable decrease and the near-bottom current velocity exceeded 20–30 cm/s.

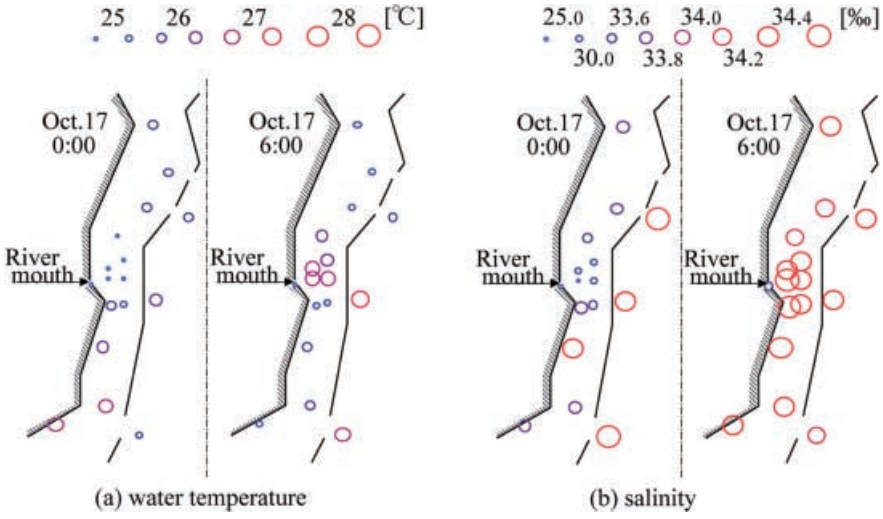

Fig. 13 Spatial distributions of water temperature and salinity and their evolution in the typhoon: **a** water temperature; **b** salinity

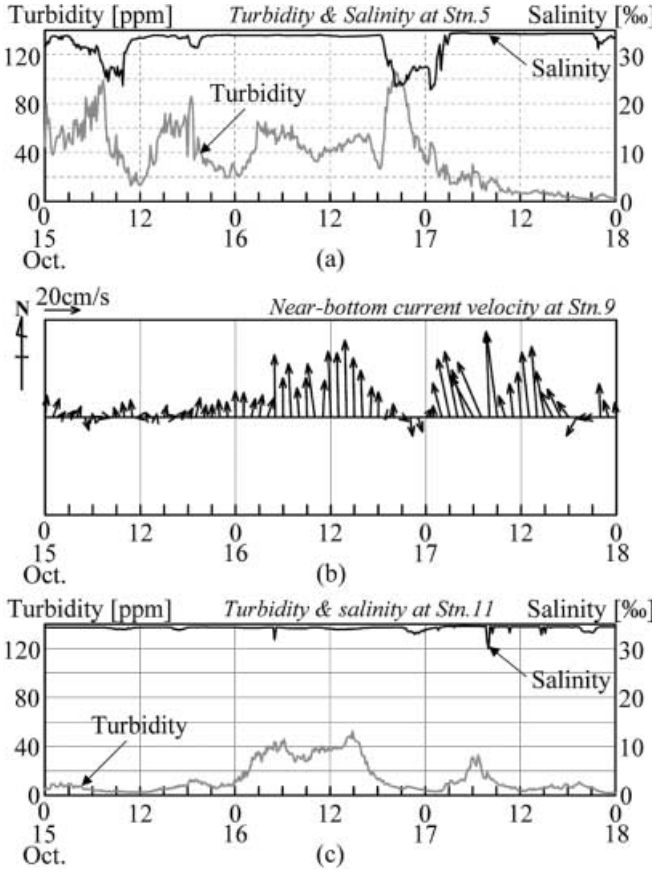

Fig. 14 Time variations of turbidity and salinity near the river mouth during the typhoon. **a** Turbidity and salinity at Stn. 5; **b** near-bottom current velocity at Stn. 9; **c** turbidity and salinity at Stn. 11

These facts suggest that the bottom sediments in this area, which are mostly fine sediments discharged from the Todoroki River and deposited in the area close to the river mouth and to the north, may be resuspended by the strong currents in the moat due to a typhoon. These resuspended fine sediments may be transported to the north in the moat and further toward the outer sea mainly through the channels at the reef edge, "Ikaguchi" and "Moriyama-guchi," indicated in Fig. 1. The sediment resuspension and subsequent transport toward the outer sea may be one of the important roles of typhoon in the sedimentary process in fringing coral reefs.

Hydrodynamic and thermal environments in the reef in normal conditions

In order to investigate the hydrodynamic and thermal environments in the reef in normal conditions, we examined the observed data for the period from 19 to 28 October.

Currents, salinity, and turbidity in the reef

Figure 15 shows the time history of the near-bottom current velocity at Stn. 9 and that of the wind velocity. In period ① indicated in the figure, an oscillating pattern is found in the velocity fluctuation, while in periods ② and ③, the northward currents prevail. The overall direction of the current coincides with the prevailing wind direction only in period ③, although the slight southward bias in the current corresponding to the wind direction is found in period ①.

Possible factors other than the wind to drive currents in the reef are tide and waves, which are to be associated with horizontal gradients of the mean water level in the reef. Figure 16 indicates the time variation of the difference between the mean water level at Stn. 1 located in the northern end of the observation area and that at Stn. 14 in the southern end, being positive when the former is higher than the latter. In period ①, the mean water level difference appears with semi-diurnal fluctuation, which corresponds to the oscillating pattern of the current velocity found in Fig. 15a; i.e., with the positive

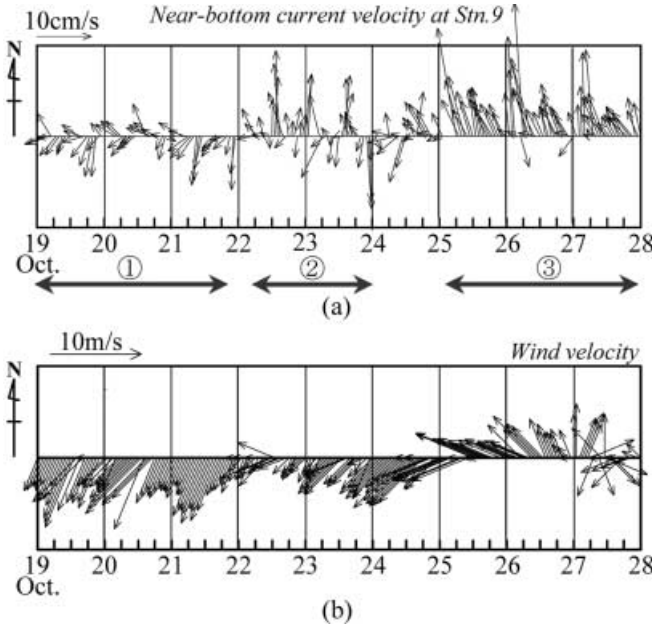

Fig. 15 Time variations of current and wind velocities in normal atmospheric conditions. **a** Near-bottom current velocity at Stn. 9; **b** wind velocity vectors

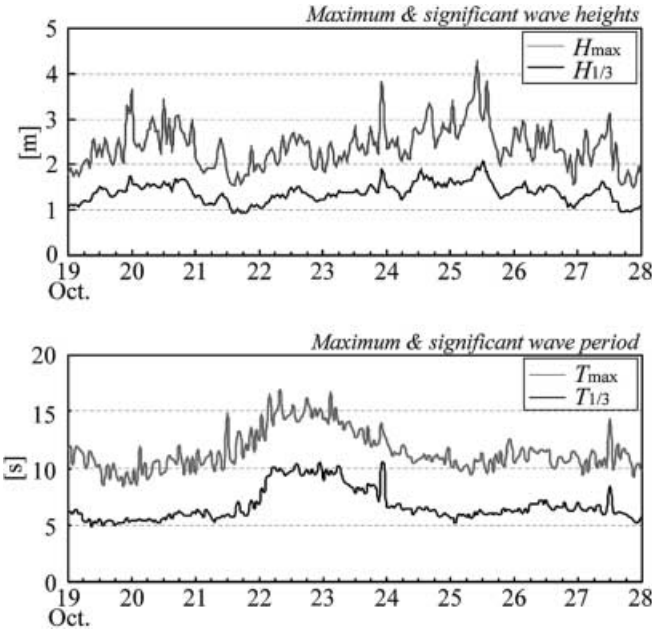

Fig. 17 Characteristics of ocean waves: *above* maximum and significant wave heights *below* maximum and significant wave periods

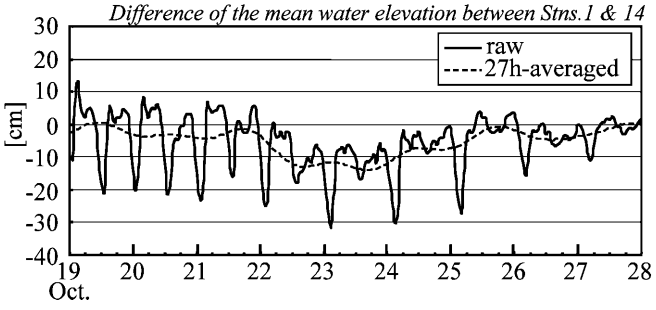

Fig. 16 Difference of mean water elevation between Stns. 1 and 14

along-shore difference in the mean water levels at high tide, the current flows to the south, and vice versa. These facts indicate that the oscillating flow pattern in period ① was derived by the semi-diurnal tidal fluctuation of the along-shore gradient of the mean water level.

In period ②, the 27-h-averaged water level difference, which is also indicated in Fig. 16, is negative with the magnitude more than 10 cm. This negative along-shore gradient of the mean water level is considered to cause the northward-prevailing currents in this period. The incident wave period observed at Stn. 17 was larger in period ②, although the wave height was nearly the same as compared with other periods, as shown in Fig. 17. This means that the change of the incident-wave condition to long-period swell caused the change in the mean water level distribution and corresponding current field in the reef.

Figure 18 shows the time variations of the near-surface salinity and turbidity at Stns. 5 and 11 in the moat located respectively in the north and south of the river mouth. On 24 and 25 October, a noticeable decrease in the salinity and increase in the turbidity occurred due to a flood. In period ②, the salinity decrease appeared at both measuring stations. By comparing with Fig. 16, we can see that the phase of the salinity decrease and the lag between Stns. 5 and 11 are correlated with the fluctuation of the along-shore gradient of the mean water level. In period , in which the northern current prevailed, the salinity decrease appeared only at Stn. 5, suggesting a deflection of the river plume to the north in the reef. Similar features can be found in the turbidity fluctuation.

All these facts described in this section demonstrate the crucial importance of the combined effects of wind, tide, waves, and river plume on the hydrodynamics in the reef and hence on the transport of the salinity and turbidity.

Thermal environments

Figure 19 shows the time variation of the 25-h-averaged water temperatures at the outer sea (Stn. 17), the river mouth (Stn. 8), and all other measuring stations in the reef. The water temperatures in the reef appeared with appreciable non-uniformity up to 1.5 °C on 19 October, but they became nearly the same on 23 October. To examine the mechanism of the appearance of these features of the 25-h-average temperature in the reef, we have made a heat-budget analysis, which is similar to that for the typhoon period, for the entire period of the observation. The results of the analysis indicate that the heat budget in the reef was governed by both the heat

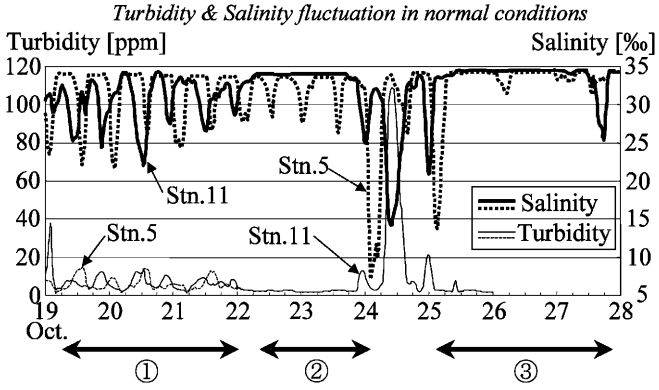

Fig. 18 Fluctuations of salinity and turbidity in normal conditions

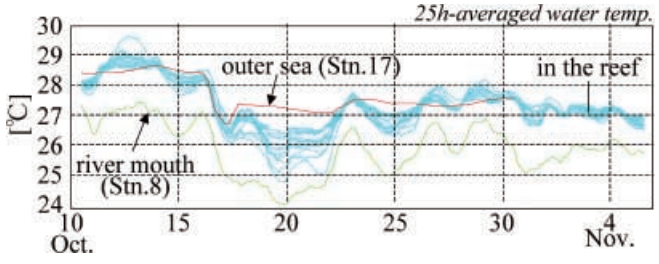

Fig. 19 Twenty-five-hour-averaged water temperature at all measuring stations

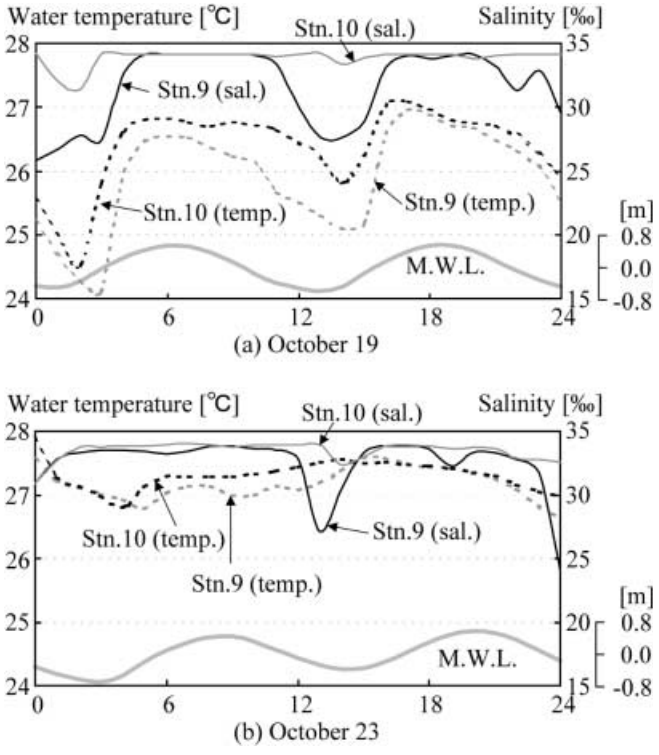

Fig. 20 Time histories of water temperature and salinity in the reef: **a** 19 October, non-uniform temperature in the reef; **b** 23 October, nearly uniform temperature in the reef

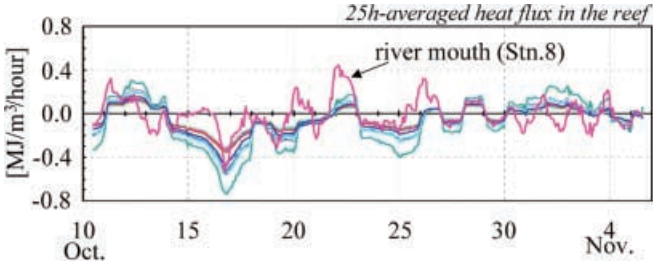

Fig. 21 Twenty-five-hour-averaged heat flux through the water surface in the reef

flux through the water surface G and the horizontal advective flux ΔF.

Figure 20 shows the time variations of the depth-averaged temperature, the near-surface salinity, and the mean water level at Stns. 9 and 10 on 19 and 23 October. In the case of the non-uniform temperature in the reef observed on 19 October, the temperature rises with the mean water level, indicating the intrusion of the outer sea water having higher temperature during the flood tide. At low tide, the temperature decreases with the salinity, showing the influences of the river plume, which is lower both in temperature and salinity. At Stn. 10 located closer to the reef edge, the water temperature is always higher than that at Stn. 9 situated near the river mouth; the temperature difference at low tide is about 1 °C. On the other hand, on 23 October, the temperature difference is small.

On 19 October and earlier, the reef water was subjected to atmospheric cooling, as shown in Fig. 21, which represents the 25-h-averaged heat flux through the water surface in the reef. The cooling is more effective in the reef than the outer sea, because of the very shallow water depth, resulting in the larger difference in the water temperature between inside and outside the reef. Besides, the river water temperature remained lower during the entire period. Therefore, during flood tide, at the locations where the effects of the outer sea water are more prominent, the water temperature may show a larger increase. On the other hand, at the locations close to the river mouth, the temperature exhibits a larger decrease especially at low tide. These characteristics are attributable to the appreciable non-uniformity of the water temperature in the reef. On 23 October, on the contrary, the atmospheric heat flux was positive, and the water temperature difference between inside and outside the reef was negligibly small, as shown in Fig. 19. This is considered the main reason for the appearance of nearly uniform temperature in the reef.

We then attempted to examine the overall feature of the atmospheric flux and the horizontal advective heat flux and their relative importance for the three different conditions; i.e., the typhoon condition from 15 to 17 October, the appreciable non-uniform temperature condition on 19 October, and the abrupt temperature increase condition on 22 October. For these purposes, we introduced a thermal control volume defined by the

shoreline, the reef edge line, and two reef-cross lines passing through Stns. 1 and 15, and evaluated the heat fluxes through the water surface and the sea bottom, the heat discharge from the Todoroki River, the temporal change rate of the heat storage, and the horizontal advective flux computed as the residual in the heat balance among these quantities.

Figure 22 summarizes the estimated values of the atmospheric heat flux through the water surface and horizontal advective heat flux at these three conditions. This figure shows that, in the typhoon condition, the reef water was cooled by the atmospheric effect at the rate of about 2.5 °C day^{-1} m^{-3}, but was warmed by the horizontal advective flux at the rate of about 1.7 °C day^{-1} m^{-3}. Since this positive horizontal advective heat flux is considered mainly due to the heat exchange with the relatively warmer water in the outer sea, we can conclude that the outer sea water may act to mitigate the atmospheric cooling of the reef water during the typhoon. In the appreciable non-uniform temperature condition on 19 October, the atmospheric heat flux and the horizontal advective heat flux are negative and positive, respectively, like those for the typhoon condition, but with less magnitude. On the contrary, on 22 October showing the rapid temperature increase in the reef of more than 1.5 °C, both the atmospheric and advective heat fluxes are positive, with larger magnitude in the latter.

Conclusions

To investigate the hydrodynamic and thermal environments of a fringing coral reef under possible influences both from inland and offshore, we conducted a field survey along Shiraho coast on Ishigaki Island, Okinawa, Japan, by deploying 16 moored buoys in and off the reef, on which various sensors for continuous measurements of water temperature, salinity, and turbidity concentration were installed. Several bottom-mounted current meters and wave gauges were also deployed.

The main conclusions of the present study are as follows:

1. During a typhoon, an abrupt change with decrease and subsequent increase in the water temperature was observed both inside and outside the reef, the resultant temperature being more than 1 °C lower than before. A corresponding abrupt change in the salinity was also observed outside the reef. These abrupt changes were considered due to the coastal up- and downwelling during the typhoon. [Regarding the cooling effect of typhoon on the reef water body, it should be noted that in summer 1998, the number of typhoons that approached the Ryukyu Islands was very few. This may be one of the additional causes of the appearance of the high-temperature anomaly in the Ryukyu Islands in summer 1998 (Nakaza et al. 1999).]
2. A heat-budget analysis for the typhoon condition revealed that the temperature-change rate outside the reef was dominated by the horizontal advective heat flux, while in the reef, the cooling effect by the atmospheric heat flux through the water surface was also significant. The horizontal advective heat flux in the reef showed appreciable variability with the difference in the location, suggesting that the influence of the outer sea water as well as the river plume appear with significant non-uniformity in the reef.
3. The overall characteristics of currents in the reef, in normal atmospheric conditions, were found to be governed by the dynamic balance among tide, waves, wind, and river plume effects, and have close relationship with the salinity and turbidity variations.
4. A heat-budget analysis performed to find thermal environments in the reef in normal conditions indicated that they were influenced by both the atmospheric conditions and the temperature difference between inside and outside the reef.

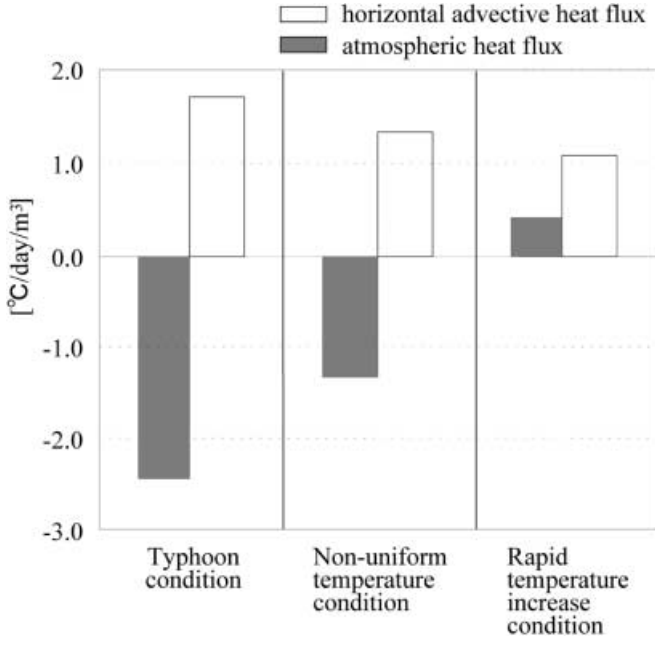

Fig. 22 Comparison of overall heat-flux components among the typhoon and two normal atmospheric conditions

Acknowledgements This study was partially supported by the Ministry of Education, Science, Sports and Culture, Grant-in-Aid for Scientific Research (B) (no. 10450181) and International Scientific Research (no. 09044144). The authors would like to thank graduate students, Mr. Tamua and Mr. Hanada, for helping with the figures and tables.

References

Andrews JC, Pickard GL (1990) The physical oceanography of coral-reef systems. In: Dubinsky Z (ed) Ecosystems of the world, vol 25. Coral reefs. Elsevier, Amsterdam, pp 11–48

Hasegawa H, Ichikawa K, Kobayashi M, Kobayashi T, Hoshino M, Mezaki S (1999) The mass-bleaching of coral reefs in the

Ishigaki Lagoon, 1998 (in Japanese). Galaxea J Jpn Coral Reef Soc 1:31–39

Kayanne H, Suzuki A, Saito H (1995) Diurnal changes in the partial pressure of carbon dioxide in coral reef water. Science 269:214–216

Kuroyama J, Nakajima T, Tsutsui H, Yoshizama T (1999) Observed situation of coral reef environments at Sekisei-shoko and influence of typhoon (in Japanese). In: Proc Trans Spring Meeting of Oceanographical Society of Japan, 27–31 March, Tokyo

Nakamori T, Suzuki A, Iryu Y (1992) Water circulation and carbon flux on Shiraho coral reef of the Ryukyu Islands, Japan. Cont Shelf Res 12:951–970

Nakaza E, Tsukayama S, Sunagawa Y (1992a) Tidal current, waves and surf beat in an area with strong near-shore currents (in Japanese). Proc Coast Eng Jpn Soc Civil Eng 39:241–245

Nakaza E, Tsukayama S, Tanaka S, Yasuzato K, Arikawa Y (1992b) A field observation of long waves and time-dependent near-shore currents in a surf zone (in Japanese). Proc Coast Eng Jpn Soc Civil Eng 39:191–195

Nakaza E, Tsukayama S, Tanaka S (1994a) A study on waves and surf beat in a reef coast (in Japanese). Proc Coast Eng Jpn Soc Civil Eng 41:86–90

Nakaza E, Tsukayama S, Sunagawa Y, Kaneshiro F (1994b) A study on red-silt deposition and diffusion in a coral reef (in Japanese). Proc Coast Eng Jpn Soc Civil Eng 41:1031–1035

Nakaza E, Tukayama S, Kawamitu Y, Sunagawa K, Kitamura Y, Kawakami K (1999) Bleaching of corals in sub-tropical area, south-west islands of Japan (in Japanese). Proc Coast Eng Jpn Soc Civil Eng 46:1236–1240

Okinawa Environmental Technology Association (1996) Report on preservation of coral reef ecosystem (in Japanese). Okinawa Environmental Technology Association, Okinawa

Omija T (1996) Effect of accumulated reddish soil on coral coverage (in Japanese). Annu Rep of Okinawa Prefectural Institute of Health and Environment, vol 30, pp 79–86

Research Institute for Subtropics (1999) Report on feasibility of subtropical studies in bio-environmental research fields – a case study on coral bleaching (in Japanese). Research Institute for Subtropics, Naha, Okinawa

Tanimoto S, Nakano Y, Ootsuki K, Uta T, Kubo A (1988) A field observation of waves and currents in Nakadomari reef area in the Okinawa Island (in Japanese). Proc Coast Eng Jpn Soc Civil Eng 35:207–211

Tsukayama S, Nakaza E, Takara N, Yara A (1992) Occurrence of the red-silt inflow and diffusion in a coral reef (in Japanese). Proc Coast Eng Jpn Soc Civil Eng 39:945–949

Wolanski E (1994) Physical oceanographic processes of the Great Barrier Reef. CRC Press, Boca Raton

Yamano H, Kayanne H, Yonekura N, Nakamura H, Kudo K (1998) Water circulation in a fringing reef located in a monsoon area: Kabira Reef, Ishigaki Island, southwest Japan. Coral Reefs 17:89–99

Yamazato K (1999) Coral bleaching in Okinawa, 1980 vs 1998. Galaxea J Jpn Coral Reef Soc 1:83–87